Physics Based Simulation Model for the Future Combat System (FCS) Non-Line of Sight Cannon (NLOS-C)

Bahram Fatemi, Mike McCullough, Cal Smith, Jayant Ramchandani and Jerry Chang
Engineering Analysis Simulation and Test
United Defense, LP GSD
San Jose, CA USA

bahram.fatemi@udlp.com

ABSTRACT

There is an increasing emphasis to reduce the weight of future ground combat vehicles due to the rapid deployment requirement that the Army is facing today. The lethality requirement for future ground combat vehicles is also increasing. To address this, one must use larger caliber weapons, increase the rate of fire, and use smart ammunition. Firing a large caliber gun on a small light/medium weight vehicle creates an engineering challenge. There are multiple competing design issues that need to be considered to make sure that the safety of the equipment and the crew is not compromised. Some of the issues to be considered are: vehicle stability, structural integrity of the vehicle chassis and its interface with the weapon subsystem, and acceleration and shock levels experienced by the crew and electronic components during the gun firing events. This paper describes how Modeling and Simulation (M&S) has been used to address these issues for the Non-Line Of Sight Cannon (NLOS-C) vehicle.

The (NLOS-C) is one of the Manned Ground Vehicles (MGV) elements of the Army's Future Combat System (FCS) program. United Defense is the prime contractor for the design and development of this vehicle. NLOS-C has a requirement for firing a 155mm cannon on a vehicle that must weigh around 20 tons. To address the challenges associated with this design, United Defense is utilizing a detailed physics based Modeling and Simulation approach. This paper concentrates on details of UDLP's physics based modeling and simulation in support of the NLOS-C vehicle.

A high fidelity dynamic model of the vehicle was developed. The Dynamic Analysis and Design System (DADS) computer program was used to develop this model. The vehicle model consists of the vehicle chassis, its suspension characteristics, and gun firing impulse load. The model was used to evaluate the vehicle stability, and shock and vibration environment before actual test firing. The model was also used to evaluate and identify the need for potential "stabilizers" during the firing event. Loads generated from this dynamic model were used as input to a Finite Element Analysis (FEA) model for structural integrity evaluations. Model validation with test data is an essential step in developing a reliable modeling and simulation tool. The test data collected in cooperation with Yuma Proving Ground, consists of platform dynamic response data for a special purpose NLOS-C demonstrator vehicle fabricated for this purpose. Good correlation with test was demonstrated, thus validating the tool for predictions of the platform firing dynamic response for the various design excursions necessary for system engineering trade studies, common subsystem integration and FCS System of System (SoS) level modeling, simulation and analysis.

Figure 1 is a picture of the NLOS-C demonstrator vehicle during a recent firing test at Yuma Proving Ground. Figure 2 is a representation of the DADS dynamic model.

Paper presented at the RTO AVT Symposium on "Functional and Mechanical Integration of Weapons and Land and Air Vehicles", held in Williamsburg, VA, USA, 7-9 June 2004, and published in RTO-MP-AVT-108.

Figure 1: NLOS-C demonstrator vehicle at Yuma proving ground.

Figure 2: DADS simulation model of the NOLS-C vehicle.

1.0 INTRODUCTION

The NLOS-C System Firing Demonstrator is designed to demonstrate the feasibility of a 155mm cannon on a Future Combat System (FCS) class vehicle. This gun is capable of 5 impulse levels of firing loads. These levels are referred to as Zones 1 through 5 with zone 1 being the lowest and 5 being the highest firing impulse. The zone value is related to the amount of propelant used for the shot.

The NLOS-C System Demonstrator employs a multitude of hardware assets that are integrated to provide a mobility and firing asset. The NLOS-C System Demonstrator is comprised of three elements: a System Demonstrator Firing Module, containing the gun firing and automated ammunition handling equipment; a Weapons Hardstand that provides the controls and electronics for the firing module, and a Surrogate Platform that provides the structure for the Demonstrator Firing Module, as well as the chassis and drivetrain to test mobility operations. Figure 3 shows the general overview of the System Demonstrator. The primary design configuration was the stabilized gun-firing configuration, with later instructions to determine if unstabilized shots were feasible. Stabilized refers to rigid structural members which support the hull to the ground, by-passing the suspension.

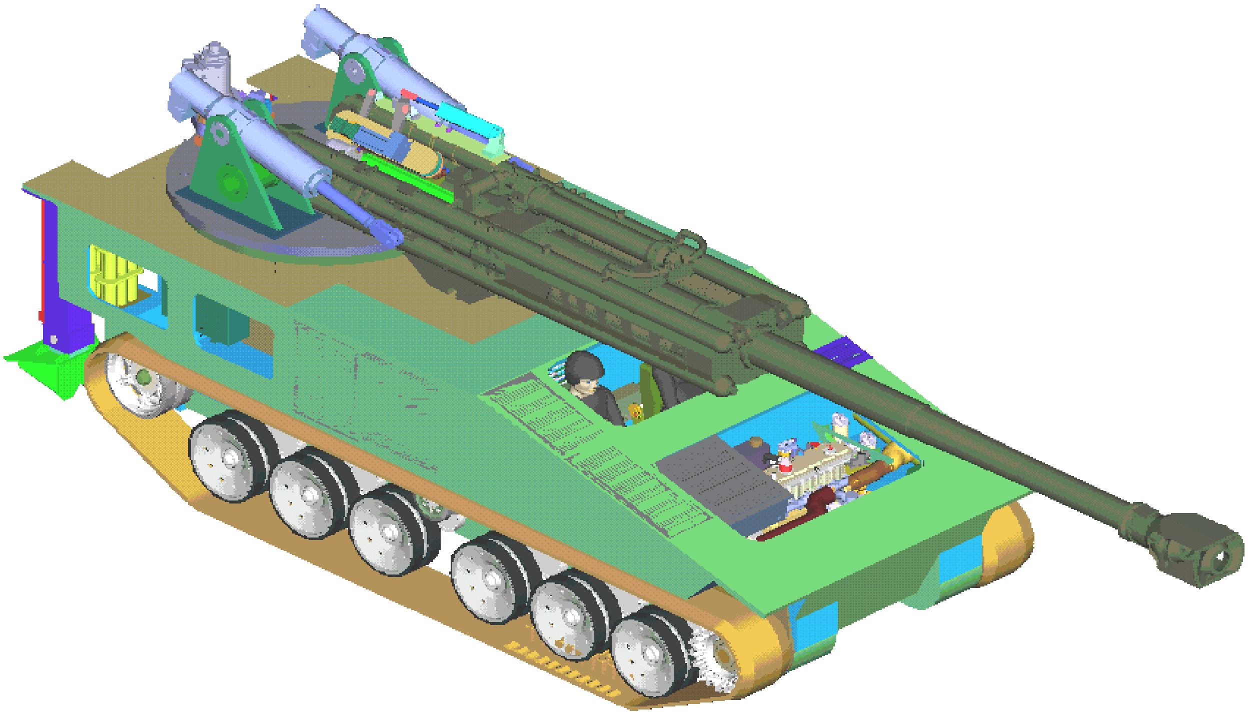

Figure 3 NLOS-C System Demonstrator Isometric View

The gun subsystem (Figure 4) consists of a modified XM777 Cannon Assembly, a Gun Mount Assembly, a Propellant Ignition Assembly, and an Automated Cannon Cleaning System (ACCS) Assembly.

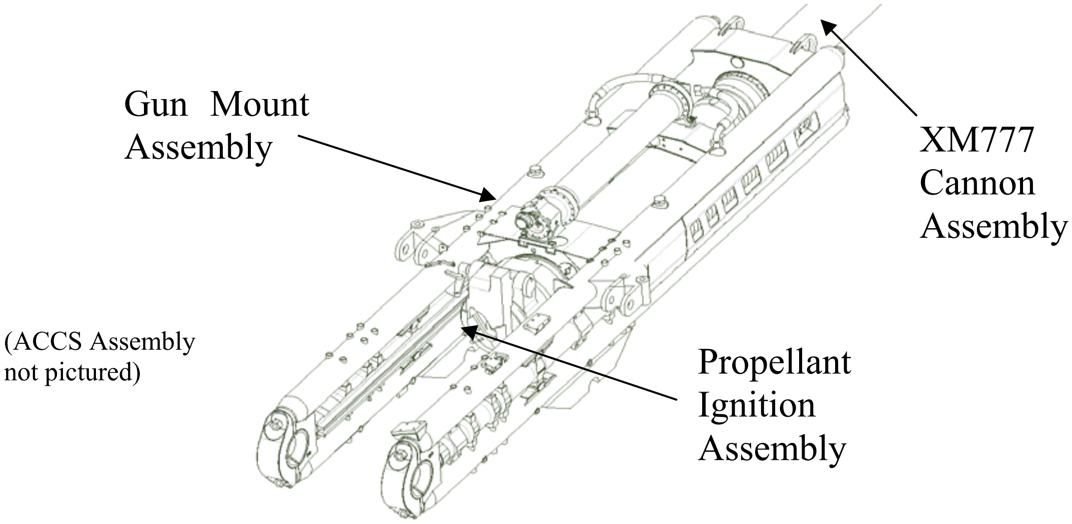

Figure 4 XM777 155mm Cannon and Gun Mount Breech Assembly

The System Demonstrator utilizes the existing XM777 screw-style swing-breech design that opens and closes via electrically actuated hydraulics.

2. ANALYTICAL MODEL DESCRIPTION

A model of the NLOS-C Demonstrator was built using DADS (Dynamic Analysis and Design System) [1], a computer simulation tool that is used to predict the behavior of multi-body mechanical systems. Position, velocity, acceleration, and reaction forces are predicted for all the parts in the model. Analysis results are studied by constructing plots with the DADSGraph module or by animating the results in DADS Model to visualize the total system behavior.

The DADS modeling environment was most recently validated and applied to tracked vehicle design on the Crusader program, where it was used for both platform stability effects on gun pointing control system design [2] and for dynamic load prediction for structural design [3].

DADS Bodies

Five rigid bodies were used to build the model. These are the chassis, the turret, the gun, and the 2 stabilizers. The turret corresponds to the traversing mass, and the gun corresponds to the elevating mass.

The following table (Table 1) shows the relationship between the DADS bodies and the Demonstrator Subsystems. Please note, that the elevating mass has only been attributed to the Gun body in DADS. Please also note, that the masses of the Projectile Handling Subsystem and the Propellant Handling subsystem have been attributed to the chassis and not to the turret. This is because these two subsystems do not traverse in this particular demonstration vehicle.

DADS Body	Demonstrator Subsystem
Chassis	Chassis Assembly; Projectile Handling Subsystem; Propellant Handling Subsystem; Propulsion subsystem
Turret	Gun Pointing Subsystem; Ammunition Loader Subsystem
Gun	Gun Tube and Recoil Subsystems; Ammunition Rammer Subsystem

Table 1: Association between DADS Bodies and Demonstrator Subsystems

Kinematic Joints

A Bracket joint was used to model the connection between the Chassis Body and the Turret. The initial condition was set to assemble the vehicle at azimuth equal to zero degrees. In order to vary the configuration for different azimuth angles, the initial assembly condition of the bracket joint can be changed, causing DADS to assemble the model in the new azimuth orientation

A Revolute joint was used to model the connection between the turret and the gun. The joint was located at the trunion and the axis of rotation of the joint was the lateral axis. A kinematic driver was used to drive the gun body to the elevation angle desired.

A Translational joint was used to model the connection between the Chassis Body and the Stabilizers. A kinematic driver was used to define the extension of the of the stabilizers. The stroke length was parameterized.

Track and Suspension

The DADS TRACK superelement was used to model the vehicle suspension systems. The theoretical assumptions involved in this element are provided in [4]. In summary, this model element assembles the equations of motion for each of the right and left suspensions system, including track, sprocket, idler, and road arms, road wheels, and the spring and damping components such that the interrelated effects of the track and roadwheels can be defined and computed efficiently. An extensible band is looped around the sprocket, idler and road wheels, and also conforms to the terrain profile, while also generating tractive forces and applying these to chassis in a manner consistent with the loop connectivity (Figure 4). This element defines the complex force interactions of the chassis, track, road wheels, and ground. Each road arm/road wheel pair must be defined in a separate road wheel sub-element within the TRACK superelement.

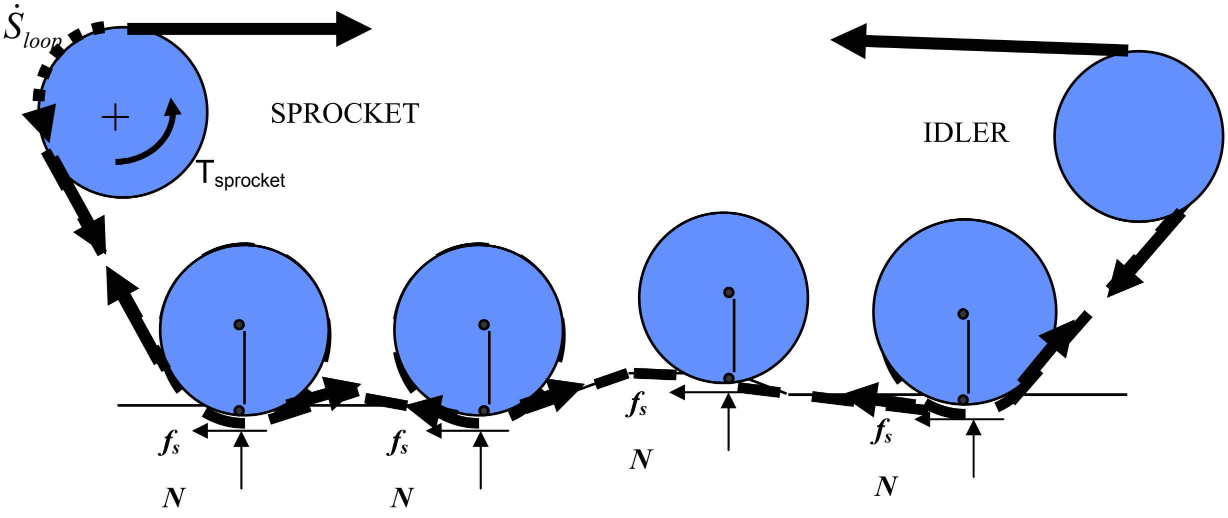

Figure 4: TRACK Superelement Bearing, Traction, Connectivity, Tension and Track Loop Definitions

The NLOS-C demonstrator was suspended on custom-built hydropneumatic suspension units (HSUs). These were respresented in the model using translational non-linear springs and dampers defining the equivalent vertical load versus vertical displacement, at the roadwheel center. The HSU spring effects differ according to rate of loading, with the extremes being governed by the adiabatic process that occurs during rapid wheel movements, and the relatively slower movements more accurately modeled using curves reflecting an isotropic compression/expansion cycle. Bump Stops were also modeled both for jounce and rebound.

Road Element

The track/ground interaction model was defined using the ROAD element. Referring to Figure 4 above, this element along with the TRACK superelement, defines the bearing forces ***N*** associated with track-ground interaction based on the classic Terramechanical bearing capacity equations [5] of the form:

$$p = \left(\frac{k_c}{w} + k_\phi \right) z^n$$

where p is the bearing pressure, z is the track pad sinkage into the original terrain profile, w is the track width, and k_c, k_ϕ and n are the coefficients and exponent required to fit experimental data for any soil and track pad combination. The sinkage is computed at a single point directly beneath each road wheel. The force acting on each road wheel is assumed to be equal to the pressure associated with the computed sinkage acting over an area equal to the track width times a wheel-ground contact patch length, h, nominally defined as one track pad length.

Tractive forces, f_s , are a function of the amount of track slip beneath each wheel. The slip velocity is the difference between the track loop velocity, and the velocity of the wheel center. Since soil shear is the operative mechanism determining tractive forces, the Baladi and Rohani equation [6] for soil shear stress development is used:

$$\tau = \frac{G\Delta\tau_{\max}}{\tau_{\max} + G|\Delta|}$$

where the Mohr-Coulomb failure criteria defines the ultimate stress at failure,

$$\tau_{\max} = c + \sigma \tan\phi$$

In these equations, G is the soil shear modulus, c is the soil cohesive strength, and ϕ is the soil internal friction angle. The track tension distribution is determined then by the tare tension in the upper strand of track, the torque on the sprocket, and the tractive forces beneath each segment. Since the model is 3-D, this equation applies to both longitudinal and lateral slip, and the resultant traction force is actually a vector quantity, with saturation limits nominally described by the friction circle.

Gun-Firing Impulses

The vehicle was designed to withstand a zone 5 impulse in the stabilized configuration. The impulses for the various zones were modeled as a percentage of the zone 5 impulse. Both the peak force and duration of the impulse were varied from that of zone 5 to achieve the impulses for zones 1 through 4. Two parameters were defined for this: these were “fire-time”, which scaled the duration of the zone 5 impulse, and “fire” which scaled the magnitude of the impulse. The table below (Table 2) shows the impulse values relative to the maximum zone 5 impulse.

When instructions were received to determine if firing in the unstabilized configuration was feasible, a trade study was performed. This trade study was done to determine the maximum gun-firing load, which could be fired before the structure, suspension or ground contact would limit it. The results showed that at zones greater than a zone 3, firing would cause the vehicle to impact the ground in the rear. Unstabilized gun firings were therefore limited to zone 3.

	Impulse as % of zone 5
Zone1	40.32
Zone2	60.66
Zone3	64.80
Zone4	85.12
Zone5	100.00

Table 2: Gun Firing Impulses

Elevation Drive Force

A Translational Spring Damper Actuator (TSDA) DADS element modeled the Elevation Drive Force. The TSDA was modeled between the Turret Elevation Clevis on the Turret Body and the Gun Tube Elevation Clevis on the Gun body.

The free length of the spring was based on the following parameters: the location of the Turret Elevation Clevis and the Gun Tube Elevation Clevis, and the elevation angle of the gun. The stiffness of the elevation drive was also parameterized. The elevation drive forces were an important result of the simulation. For example, it was used to determine if the modified XM777 was within its structural limits. The DADS simulation results indicated that the modified XM777 required added structure.

Stabilizer/Soil Interaction

The stabilizer soil interaction was modeled using Tire Force elements. Since the tire element calculates only forces, there are no constraints added by this element. Three components of force are calculated with respect to the ground surface: normal, longitudinal, and lateral. These forces are calculated in the tire/ground interface plane and then transformed to the global coordinate system when appended to the body to which the tire is attached. Used in this way this model element is essentially a point follower contact element. The ground contact stiffness and damping were linear parameters in the model.

3. VEHICLE INSTRUMENTATION

The table below (Table 3) enumerates the gauges, which were used for the correlation. The main gauges used for the rigid body simulation were the sonars and accelerometers at the four corners. Preliminary comparisons were done with the Crew Compartment accelerometers – however, this was subsequently removed from the correlation because there were some data capture issues with this channel. In addition, some lower frequency structural modes, which fall outside the purview of rigid body dynamics are not captured in the simulation and therefore correlation with test does not match well. For the structural analysis the strain gauge data was used.

ID	Type	Description
CTD016	Sonar	Vehicle Front Left Corner
CTD017	Sonar	Vehicle Front Rt Corner
CTD018	Sonar	Vehicle Rear Left Corner
CTD019	Sonar	Vehicle Rear Rt Corner
CTD021	Accel	Crew Compartment (X)
CTD022	Accel	Crew Compartment (Y)
CTD023	Accel	Crew Compartment (Z)
CTD028	Strain	L Flange Trunnion Mt
CTD030	Strain	R Flange Trunnion Mt
CTD044	Accel	Veh Front Left Corner
CTD045	Accel	Veh Front Rt Corner
CTD046	Accel	Veh Rear Left Corner
CTD047	Accel	Veh Rear Rt Corner
CTD049	Strain	Sticker Chamber
CTD051	Strain	Pin, Left

Table 3 Gauge Data used in Correlation study

4. INITIAL CORRELATION

Initial Correlation was performed for the following rounds:

- Stabilized Configuration: Zones 1 through 5, low, mid and high Quadrant of Elevation (QE)(total 15 rounds)

- Unstabilized Configuration: Zones 1 through 3; low, mid and high QE (total 9 rounds)

The displacement data along the vertical axis at the four corners (Sonar data), as well as the accelerometer data at the 4 corners of the vehicle were compared between simulation and test.

The test data was sampled at a frequency of 10 KHz. The test data was further filtered by a low frequency, 50 Hz, 3rd order, Butterworth filter. The following Matlab filter design commands were used to define the filter:

```
order = 4;

cutoff = 50;

nyquist = 5000;

[b,a]=butter(order,(cutoff/nyquist),'low');
```

Initial Correlation of Stabilized Rounds

The following table (Table 4) summarizes the correlation for Zone 5 stabilized, low, mid and high QE's. This correlation is representative of all stabilized rounds. For the stabilized rounds the peak amplitude was used as a measure of displacement as opposed to the total excursion. When the stabilizer-ground model is refined the total excursion can be used as a measure.

Please note, a negative percentage implies that the simulation under-predicts the test; and a positive implies over-prediction.

		Peak Displacement (inches)			Peak Acceleration (g's)		
QE	Round	Test	Simulation	Percentage Difference	Test	Simulation	Percentage Difference
Low	159	9.7	6.12	-36.91%	2.74	3.2	16.79%
Mid	156	3.76	3.47	-7.71%	2.08	2.61	25.48%
High	155	0.93	0.87	-6.45%	1.43	1.54	7.69%
Average				-17.02%			16.65%

Table 4 Initial Correlation of Stabilized Rounds

Initial Overlays for Stabilized Rounds

Figures 5 through 7 show the initial correlation for the stabilized shots for low to high elevation angles.

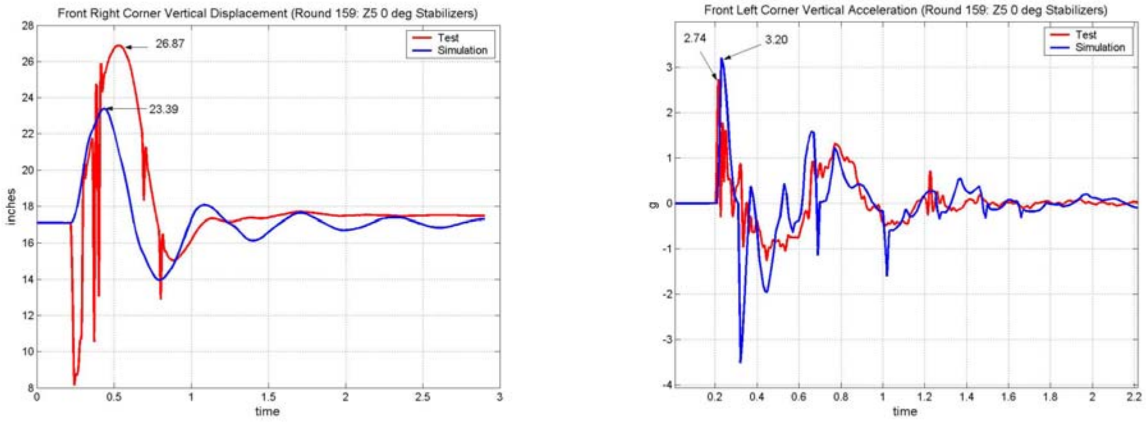

Figure 5 Initial Correlation – Corner Peak Displacement & Peak Acceleration Round 159, Zone 5, Low QE, Zero Azimuth, With Stabilizers

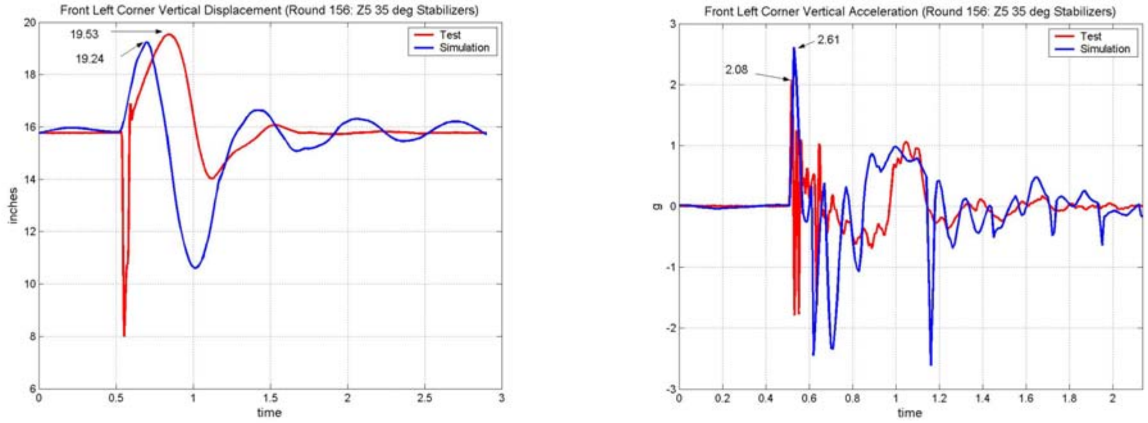

Figure 6 Initial Correlation – Corner Peak Displacement & Peak Acceleration Round 156, Zone 5, Mid QE, Zero Azimuth, With Stabilizers

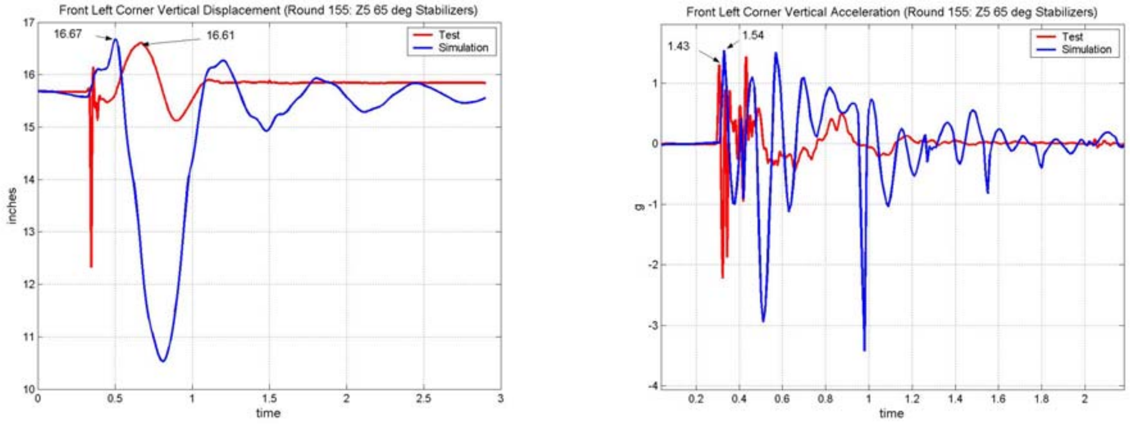

Figure 7 Initial Correlation – Corner Peak Displacement & Peak Acceleration Round 155, Zone 5, High QE, Zero Azimuth, With Stabilizers

Initial Correlation of Unstabilized Rounds

The following table (Table 5) summarizes the correlation for Zone 2, unstabilized, low, mid and high QE's. This correlation is representative of all unstabilized rounds. For the unstabilized rounds the total excursion was used as a measure of displacement as opposed to the peak. This is because total excursion represents the impact of the vehicle suspension on the system response far better than the peak amplitude. Note that a negative percentage implies that the simulation under-predicts the test; and a positive implies over-prediction.

		Total Excursion (inches)			Peak Acceleration (g's)		
QE	**Round**	**Test**	**Simulation**	**Percentage Difference**	**Test**	**Simulation**	**Percentage Difference**
Low	92	19.6	9	-54.08%	0.88	0.94	6.82%
Mid	85	19.46	9.5	-51.18%	0.83	0.85	2.41%
High	88	17.2	13.82	-19.65%	0.64	0.91	42.19%
Average				-41.64%			17.14%

Table 5 Initial Correlation of Unstabilized Rounds

Initial Overlays for Unstabilized Rounds

Figures 8 through 10 show the initial correlation of unstabilized shots for low to high elevation angles.

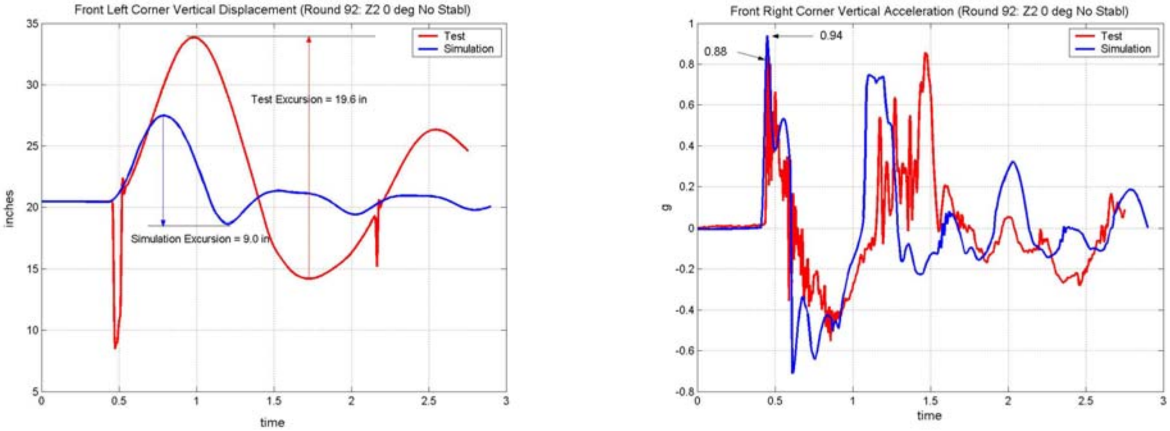

Figure 8 Initial Correlation – Corner Displacement & Acceleration
Round 92, Zone 2, Low QE, Zero Azimuth, Without Stabilizers

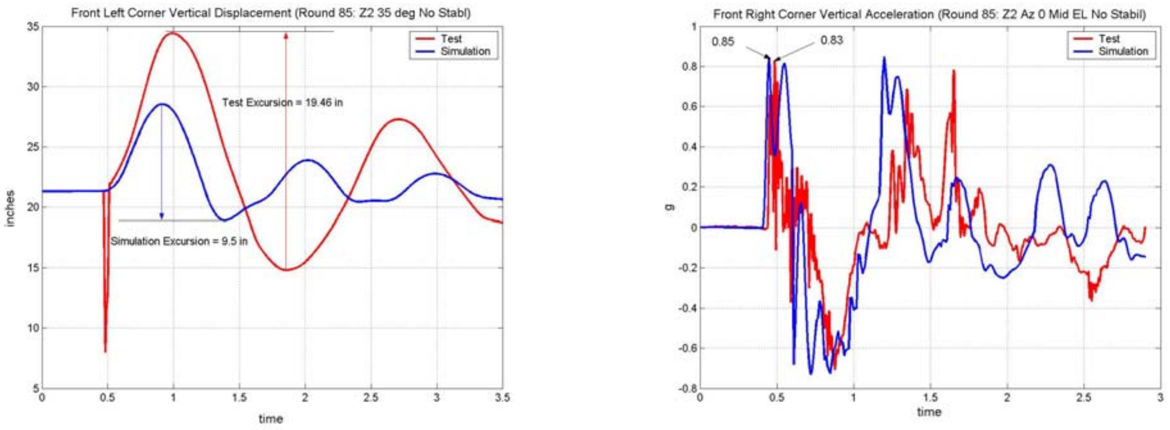

\

Figure 9 Initial Correlation – Corner Displacements & Acceleration Round 85, Zone 2, Mid QE, Zero Azimuth, Without Stabilizers

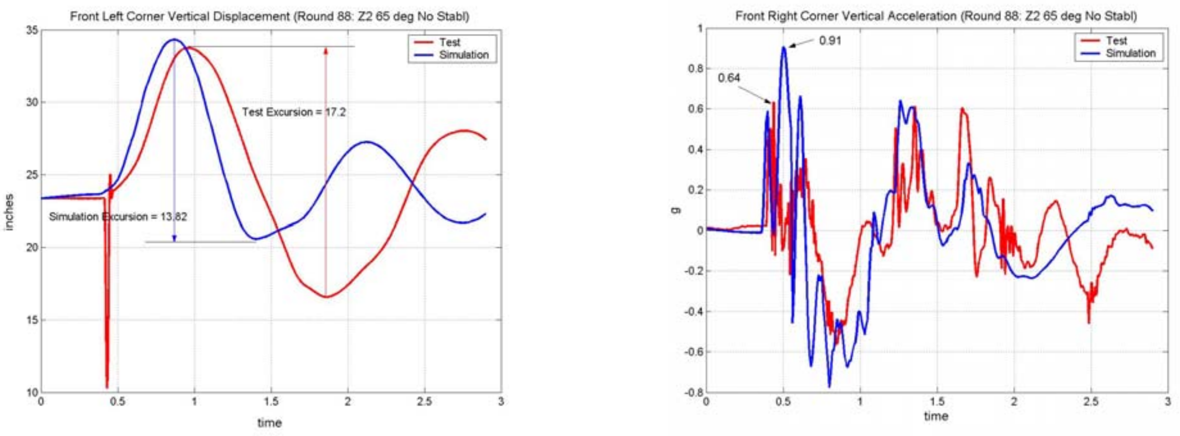

Figure 10 Initial Correlation – Corner Displacements & Acceleration Round 88, Zone 2, High QE, Zero Azimuth, Without Stabilizers

4. MODEL REFINEMENT BASED ON TEST CONFIGURATION ADJUSTMENTS

Several model iterations were made in order to improve the fidelity of the simulation. The iterations included adding a rifling torque, performing sensitivity studies on the mass properties (mass, inertias and cg location), changing the track tension, modifying the suspension, changing the road properties. Not all the model iterations were incorporated. For example the rifling torque was not incorporated. This rifling torque was initially considered because the rounds fired with the stabilizers emplaced showed some roll. However, since the unstabilized rounds did not evidence any roll the rifling torque was removed. The roll was then attributed to a minor difference in the stabilizer-ground reactions between the left and right.

However, there were some model changes which could be justified based on empirical observations and which had a significant impact on the simulation results. These changes were incorporated in the improved model. They are discussed in the sections below.

Impulse Calculations

In order to increase the accuracy of the impulse force, gun recoiling data captured from the high-speed video of an unstabilized round was used. This was done with the gun at the mid elevation position. From this data, the position time history of the recoiling mass was captured. The position data was twice differentiated to get the acceleration of the recoiling mass. The inertial force of the recoiling mass was then used as the impulse imparted to the demonstrator. Figure 11 depicts the acceleration of the recoiling mass for Zone 2. This was a much more accurate depiction of the impulse forces than the original calculation. The original calculations were based on muzzle velocity, which did not take into account duration of the recoil and counter recoil strokes. High speed video was not available for the high and low angles, so the mid elevation impulse was used for all angles.

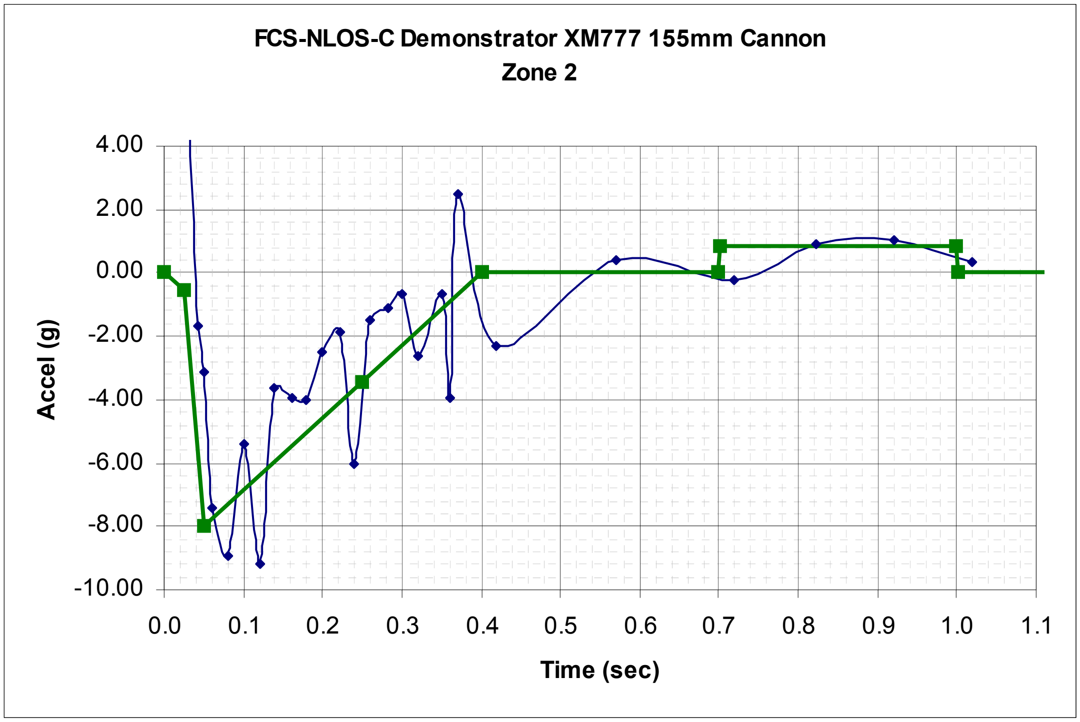

Figure 11 Recoiling Mass acceleration at Zone 2 Mid QE

Track Tension

Track tension is typically set using a catenary model of the upper track strand and measuring the sag. However, for bandtrack the catenary sag was too small, and the measurement suffered from a loss of significance errors. Therefore, the first vibration mode frequency was used to estimate track tension.

A simple experiment was set up to measure the frequency. The upper track segment between the sprocket and the center roller was excited. A pencil was attached to the track with adhesive tape. A paper was moved past the pencil. This recorded the oscillations of the track. The duration for the oscillations was determined using a stopwatch. The frequency can then used to deduce the track tension. The average frequency was about 5.5 Hz. The length of the track segment between the sprocket and the center roller was about 100 inches. Based on a simple string vibration model, the track tension was calculated to be about 6700 lbf.

Suspension

The isotropic suspension spring curves were used. In addition the slope of the spring curves were modified in order to match the heave and pitch frequencies of the vehicle. The heave and pitch data was extracted from the displacement data captured at the four corners of the vehicle. The offset of the spring curves was maintained while changing the slope.

The tables (Tables 6 and 7) below summarizes the correlation for pitch and heave frequencies for both the original model and the improved model.

	Frequency (Hz)		
	Test	**Simulation**	**Percentage Difference**
Pitch	0.58	0.95	63.81%
Heave	1.10	0.95	-13.33%

Table 6 Original Model – Pitch and Heave Frequency Correlation

	Frequency (Hz)		
	Test	**Simulation**	**Percentage Difference**
Pitch	0.58	0.59	1.78%
Heave	1.10	1.18	7.06%

Table 7 Improved Model – Pitch and Heave Frequency Correlation

The pitch and heave data has been extracted from the sonar data. Please note that the pitch reference plane is the angle made with the horizontal by the plane passing through 3 of the sonars and therefore the pitch angle at rest is not zero degrees. In addition, the points of interest in the DADS model are not exactly coincident with the sonars. Because the emphasis was on correlating the frequency, the simulation data was not post-processed to match the test offset.

The following overlays in Figures 12 though 15 show the original and improved correlation for pitch and heave frequencies from an unstabilized zone 2 round.

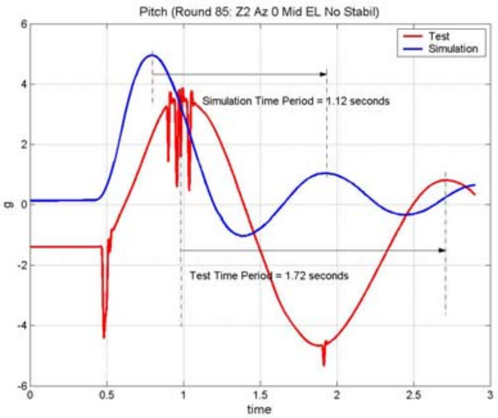

Figure 12 Original Model – Pitch Overlays

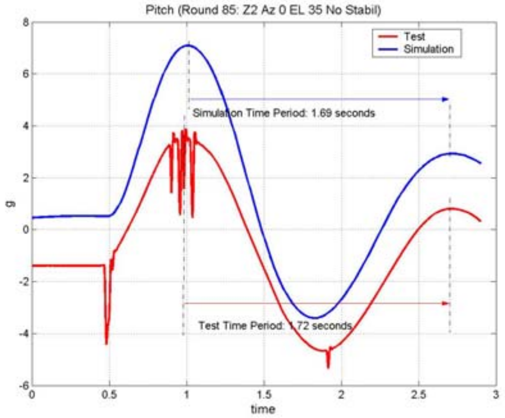

Figure 13 Improved Model – Pitch Overlays

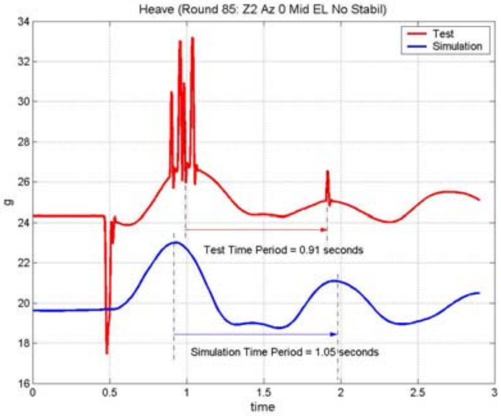

Figure 14: Original Model – Heave Overlays

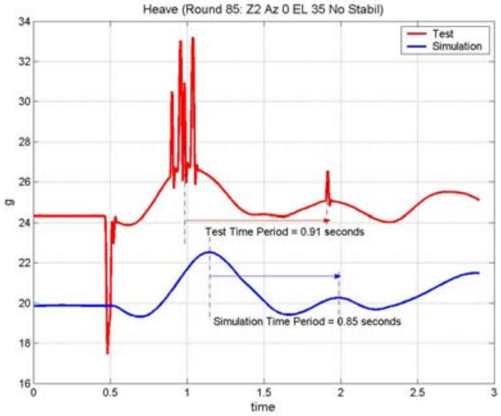

Figure 15: Improved Model – Heave Overlays

Ground Friction Properties

The most significant initial discrepancy between test and simulation was the longitudinal displacement of the chassis for the unstabilized rounds. The gun was fired with the parking brakes on, and the test showed neglible slip motion of the chassis. The model however showed 12” of motion. In order to account for this the road properties in the DADS model were changed. The shear modulus, ***G***, in the Baladi Rohani shear force equation mentioned above, which represents the slope of the friction-velocity curve, was increased ten-fold. In addition, the DADS subroutine was changed. This change was to reduce the reference value for the transition velocity at which the velocity-slip model of friction diminishes it slope to zero -- this avoids the singularity at zero. After this change, the model reduced the predicted longitudinal slippage to about ½ inch of, while increasing the pitch motion and was much more consistent with test. Note that there was no direct measurement of slip during the test. Only high-speed video results can be used to estimate the test value, and this was not done formally.

5. ADJUSTED TEST CONFIGURATION UPDATED CORRELATION

Stabilized gun firing correlation was not updated since it was within reasonable (20%) limits, and not affected substantially by the changes made to the DADS model. The stabilized model is much more controlled by the ground contact of the stabilizer, than any other parameter.

Updated Correlation for Unstabilzied Rounds

The following table summarizes the correlation for Zone 2, unstabilized, low, mid and high QE's. These results are from the simulation, which incorporates all model changes discussed above in section 6.0

QE	Round	Total Excursion (inches)			Peak Acceleration (g's)		
		Test	Simulation	Percentage Difference	Test	Simulation	Percentage Difference
Low	92	19.6	17	-13.27%	0.88	1.08	22.73%
Mid	85	19.46	20.46	5.14%	0.83	0.81	-2.41%
High	88	17.2	21.14	22.91%	0.64	0.64	0.00%
Average				4.93%			6.77%

Table 8 Final Correlation of Unstabilized Rounds

Updated Overlays for Unstabilzied Rounds

Figures 16 through 18 show the improved correlation for the stabilized shots for low to high elevation angles.

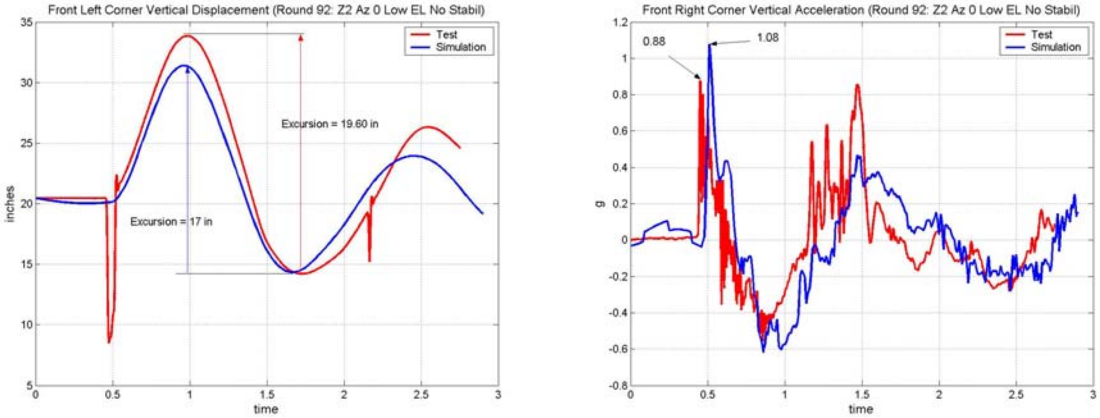

Figure 16 Updated Correlation – Corner Displacement & Acceleration
Round 92, Zone 2, Low QE, Zero Azimuth, Without Stabilizers

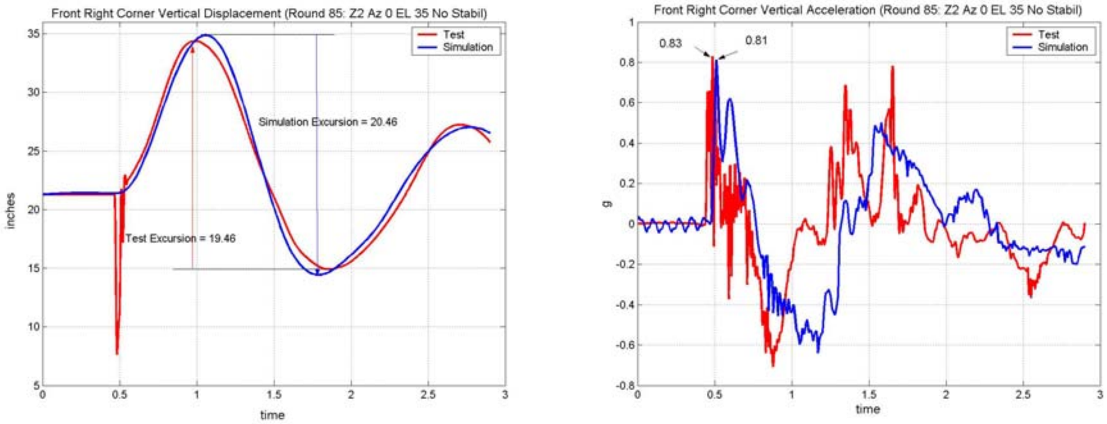

Figure 17 Updated Correlation – Corner Displacement & Acceleration
Round 85, Zone 2, Mid QE, Zero Azimuth, Without Stabilizers

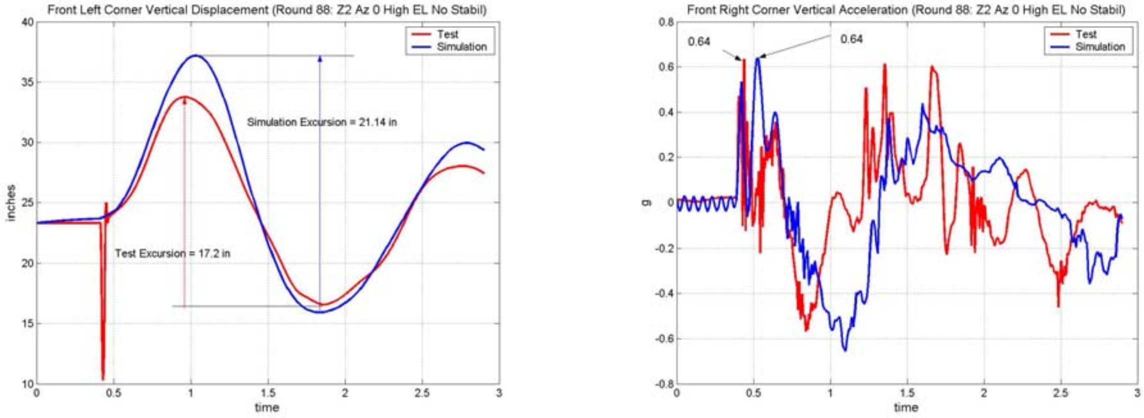

Figure 18 Updated Correlation – Corner Displacement & Acceleration
Round 88, Zone 2, High QE, Zero Azimuth, Without Stabilizers

Summary of Correlation Results

The results of the simulation have been correlated for both stabilized and unstabilized configurations. For the stabilized configuration correlation has been done with results from Zones 1 through 5. For each of these zones the low, mid, and high QE rounds have been considered. For the unstabilized configuration correlation has been done with results from Zone 1 through Zone 3. Firing unstabilized for Zones 4 & 5 was not feasible giving the systems demonstrator CG and suspension configuration.

Simulation results were correlated with sonar (displacement) and accelerometer data captured from test. Model changes were made in order to achieve better correlation for both amplitude and frequency.

The original stabilized model showed that simulation results were good, many cases within 15%. The original unstabilized model showed that simulation results under-predicted the test by about 42% for the displacement data. The simulation results also over-predicted the peak accelerations at the corners by about 17%.

In addition, the vehicle pitch and heave data was extracted from the displacement data. The original model showed that the simulation results over-predicted the pitch frequency by 64% and under-predicted the heave frequency by 13%.

The majority of the correlation effort was spent on the unstabilized model, since this is of significant importance to the unstabilized NLOS-C objective system. Several model iterations were made in order to improve the fidelity of the simulation. However, only those model changes which could be justified based on empirical observations, and which showed a significant impact on simulation results were incorporated. The following 4 model changes were incorporated (discussed in more detail in section 6.0):

- Improved impulse data based on recoiling mass accelerations captured by high-speed video
- Softer suspension springs
- Increased Ground Shear Slope near zero velocity
- Lower Track Tension

After incorporating these changes, the simulation results were significantly improved. The updated unstabilized model showed that simulation results under-predicted test by about 5% for the displacement data. The simulation results over-predicted the peak accelerations at the corners by about 7%. In addition, the improved model showed that the simulation results over-predicted the pitch frequency by 2% and over-predicted the heave frequency by 7%.

6. CONCLUSIONS

- The model produced reliable predictions of acceleration and displacement levels for stabilized operation throughout all zones and firing angles.
- The updated model is a good predictor of displacements and accelerations for the unstabilized configuration -- within 10%.
- Impulse is significantly affected by gun elevation, and should be accounted for in the analysis.
- The test data indicates progressively lower front sonar displacements as the elevation angle is increased. The model has the opposite trend and behaves consistently with expectations derived from an increasing moment arm about the platform CG. This disagreement between test and analysis may be rooted in an unmeasured variation in the firing impulse at each angle, and/or inaccuracies in the center of gravity and pitch moments of inertia.

7. REFERENCES

1. “Dynamic Analysis Design System (DADS) Reference Manual”, Version 9.6, LMS-North America, Coralville, Iowa. , October 2002
2. Johnson, Gregory S., and Stuva, Richard L., “Crusader Field Artillery System Platform Stability and Active Gun Pointing Response Analysis” SAVIAC, Minneapolis MN, October 1998.

3. McCullough, Mike K., and Khubchandani, Ashok, "Shock Load Prediction in Military Tracked Vehicles", proceedings of the 69th Shock and Vibration Symposium, Shock and Vibration Information Analysis Center, December 1999.

4. McCullough, M.K., "Terra-Dynamics of High Mobility Tracked Vehicles", Ph.D. Dissertation, University of Iowa, 1985.

5. Bekker, M.G., "Introduction to Terrain-Vehicle Systems", University of Michigan Press, Ann Arbor MI, 1969.

6. Baladi, G.Y., and Rohani, B., "A Terrain-Vehicle Interaction Model for Analysis of Steering Performance of Track-Laying Vehicles," USAE WES Tech. Rept. GL-79-6, 1979.